

## **GEOSYNTHETIC REINFORCEMENT IN LANDFILL DESIGN: US PERSPECTIVES**

**Jorge G. Zornberg<sup>1</sup>, M. ASCE**

**Abstract:** Geosynthetic reinforcement in landfill applications in the US has involved conventional reinforced soil structures and veneer stabilization with reinforcements placed along the landfill slope and anchored at the crest. In addition, innovative approaches have been recently implemented in the US to reinforce landfill covers and base liners. This includes horizontally placed geosynthetic reinforcements, which are anchored into solid waste, and fiber reinforcement to enhance the shear strength of the soil liner material and the interface shear strength between the soil liner and texture geomembranes. This paper presents a framework for the design of steep reinforced liners. Recent case histories illustrating the use of the different geosynthetic reinforcement applications are also presented to document the different approaches in specific projects.

### **INTRODUCTION**

The design of steep veneers (e.g. steep cover or base liner systems for waste containment) poses significant challenges to designers. The use of uniaxial reinforcements placed along the slope (under the veneer and over the typically strong mass of solid waste) and anchored at the crest of the slope has been a common design approach. However, this alternative may not be feasible for steep, long veneer slopes. An innovative approach recently implemented in the US involves the use of uniaxial reinforcements placed horizontally (rather than along the slope) and anchored into the waste mass. Also, the use of fiber-reinforcement has been recently used in the US for stabilization of veneers and control of desiccation cracking.

A framework for analysis and design of reinforced veneers is summarized in this paper. The framework is particularly useful for parametric evaluations and evaluation of alternatives considered when defining the reinforcement requirements for this system. The various reinforced veneer approaches can be used not only for reinforcement of landfill cover systems (placed over comparatively strong solid waste) but also for reinforcement of base liners and other veneers placed over comparatively strong subgrade material. This paper also builds on a recent review on the use of geosynthetics in waste containment facilities (Bouazza et al. 2002). The reader is referred to that source for information regarding recent use of geosynthetics in landfill design for functions other than reinforcement.

---

<sup>1</sup>University of Texas at Austin, USA

## **CONVENTIONAL REINFORCED SOIL STRUCTURES IN LANDFILL DESIGN**

### **General Approach**

As in any other geotechnical system, conventional geosynthetic-reinforced soil structures have been used in the US to stabilize earthwork systems in landfill projects. This is the case in the periphery of landfill sites, which are often constrained by the limits of the landfill property. A specific criterion not necessarily accounted for in the design of typical earth retaining structures is the need to sustain significant differential settlements. This is the case of structures founded over solid waste, which should be able to sustain major settlements without structural distress. Geosynthetic-reinforced soil structures are particularly suitable in such cases, as indicated in the case history described below. Additional cases of reinforced soil structures in landfill projects are presented by Cargill and Olen (1998).

### **Case History: Toe Buttress at OII Superfund site, Monterey Park, California**

A geogrid-reinforced toe buttress was constructed in 1987 at the OII Superfund site in order to enhance the stability of the southeastern slopes of the OII Landfill Superfund site. The toe buttress is immediately adjacent to a residential development. The waste slopes behind the toe buttress are up to 37 m high with intermediate slopes between benches up to 18 m high and as steep as 1.3H:1V. The approximately 4.6 m high, 460 m long toe buttress was built using sandy gravel as backfill material. The front of the structure was founded on concrete piers. However, as the back of the toe buttress was founded on waste, the structure had been subjected to more than 0.6 m of differential settlements since the end of its construction (Zornberg and Kavazanjian, 2001).

In response to concerns regarding the internal stability of the reinforced soil structure, finite element analyses were performed to evaluate the long-term integrity of the geogrid reinforcements under static and seismic loads. The analyses considered 40 years of settlement followed by the design earthquake. The finite element modeling evaluated the strains induced in the geogrid reinforcement considering both material and geometric nonlinearity. The analyses were performed in three sequential phases: (i) toe buttress construction, modeled by sequentially activating soil and bar elements in the reinforced soil zone; (ii) gradual increase in differential settlements, simulated by imposing incremental displacements at the base of the reinforced soil mass; and (iii) earthquake loading, modeled by applying horizontal body forces representing the maximum average acceleration estimated in a finite element site response analysis.

A total of 2.0 m of differential settlement was imposed on the base of the finite element mesh to simulate long-term differential settlement. The maximum strain in the geogrid reinforcements calculated after this long-term static loading was less than 3.0 percent, well below the allowable static strain of 10 percent. The calculated maximum geogrid strain induced by construction, long-term differential settlement, and earthquake loading was approximately 8.5 percent, well below the allowable strain of 20 percent established for rapid loading. The results of this study indicate that the integrity of the geogrid-reinforced buttress should adequately sustain additional differential settlements and earthquake loads.

Figure 1 summarizes the strain distribution in the five primary reinforcement layers of the toe buttress corresponding to the sequential phases of the numerical simulation. The figure shows the strain distribution: (i) at the end of construction (maximum strain of 0.4%), (ii) after imposing foundation settlements leading to approximately 600 mm of settlement at the back of the toe buttress (current condition, maximum strain of 1.5%), (iii) after imposing foundation settlements resulting in approximately 1,220 mm of settlement at the back of the toe buttress (long-term static condition, maximum strain of 2.9%), and (iv) after applying a pseudo-static earthquake load of 1.0 g (maximum strain of 8.5%).

These results highlight the relevance of assessing correctly the location of the critical reinforced zone. As shown in the figure, the elevations at which the maximum reinforcement strains occur in a geosynthetic-reinforced soil slope vary significantly for different loading mechanisms. The geogrid strains that develop during construction are comparatively small (less than 0.4 %). The numerical simulation indicates that the maximum reinforcement strain induced by construction loading occurs at mid-height of the reinforced slope, while that induced by differential settlements occurs towards the base of the structure, and that induced by earthquake loading occurs towards the top of the structure.

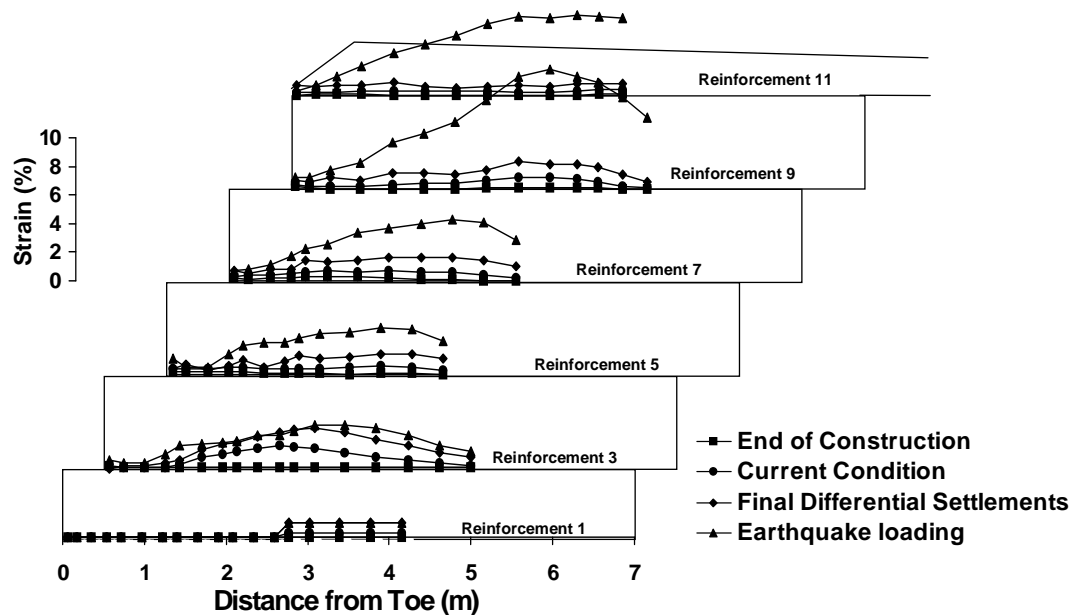


Figure 1. Estimated Geogrid Strains in the Toe Buttress Wall at the OII Superfund Site.

### STABILITY OF LINER SYSTEMS

The use of uniaxial reinforcements placed along the slope (under the veneer and above a typically strong mass of soil or solid waste) and anchored on the top of the slope has been a common approach to stabilize veneer liners. However, this alternative may not be feasible for steep, long veneer slopes. As the veneer slope rests on top of a comparatively stronger mass solid waste, alternative approaches can be considered. This includes use of uniaxial reinforcements placed horizontally (rather than along the slope) and anchored into the underlying mass. A second alternative includes the use of fiber-reinforced soil. Although

different definitions for the factor of safety have been reported for the design of reinforced soil slopes, the definition used in this study is relative to the shear strength of the soil:

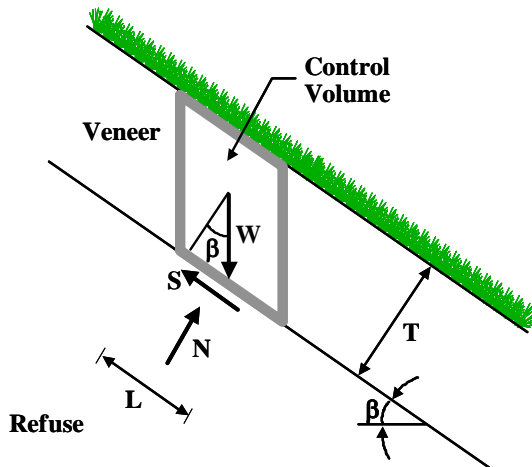
$$FS = \frac{\text{Available soil shear strength}}{\text{Soil shear stress required for equilibrium}} \quad (1)$$

This definition is consistent with conventional limit equilibrium analysis, for which extensive experience has evolved for the analysis of unreinforced slopes. Current design practices for reinforced soil slopes often consider approaches that decouple the soil reinforcement interaction and do not strictly consider the factor of safety defined by Equation 1. Such analyses neglect the influence of reinforcement forces on the soil stresses along the potential failure surface and may result in factors of safety significantly different than those calculated using more rigorous approaches. Considering the normal and shear forces acting in a control volume along the veneer slope (or infinite slope), and assuming a Mohr-Coulomb shear strength envelope, Equation 1 can be expressed as:

$$FS = \frac{c + (N/L) \tan \phi}{S/L} \quad (2)$$

where  $N$  = normal force acting on the control volume (per linear thickness);  $S$  = shear force acting on the control volume (per linear thickness);  $L$  = length of the control volume;  $c$  = soil cohesion; and  $\phi$  = soil friction angle.

Equations 1 and 2 are valid for both unreinforced and reinforced systems. In the case of an unreinforced veneer (Fig. 2), the shear and normal forces required for equilibrium of a control volume can be defined as a function of the weight of this control volume. That is:



$$S = W \sin \beta \quad (3)$$

$$N = W \cos \beta \quad (4)$$

$$W = \gamma L T \quad (5)$$

where  $W$  = weight of the control volume;  $\beta$  = slope inclination;  $T$  = veneer thickness; and  $\gamma$  = soil total unit weight. Equations 2, 3, 4, and 5 lead to the classic expression for the factor of safety  $FS_u$  of an unreinforced veneer (without considering seepage):

$$FS_u = \frac{c}{\gamma T \sin \beta} + \frac{\tan \phi}{\tan \beta} \quad (6)$$

Figure 2. Unreinforced veneer

## LINERS REINFORCED WITH GEOSYNTHETICS PARALLEL TO THE SLOPE

### General Approach

The typical method used to stabilize veneer liner systems involves a two wedge finite slope analysis. The design of these systems has been typically conducted using the

methodologies proposed by Giroud et al. (1995a) and Koerner and Soong (1998). Figure 3 shows the geometry considered in these approaches, and identifies differences in the assumptions. These approaches also differ in the definition of the factor of safety.

Giroud et al. (1995a) do not include a factor of safety at the horizontal failure surface (AB) and define the factor of safety as the ratio between the resisting and the driving forces acting on the active wedge as projected on the slope direction. The factor of safety in this solution is the sum of five separate terms, which facilitates identification of the different contributions to the stability of the slope. Table 1 presents the contribution of different parameters to the factor of safety. Giroud et al (1995b) discuss stability analysis of veneer systems considering seepage forces. The analysis presented by Koerner and Soong (1998) is consistent with the generic definition of factor of safety stated by Equation 1. Using the

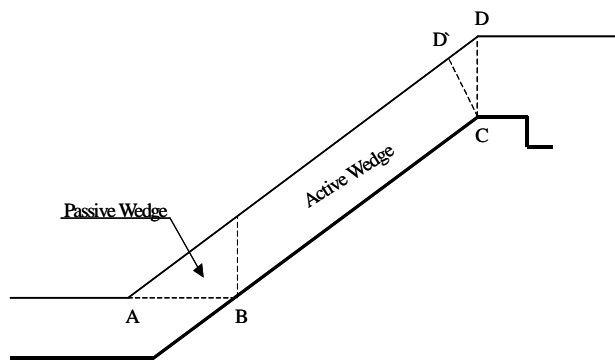


Figure 3: Schematic representation of the geometry of a cover for two-wedge finite slope analysis.

Notes: ABC = slip surface; CD = top of the cover soil as defined in the analysis by Koerner and Soong (1998); CD' = top of the cover soil as defined in the analysis by Giroud et al. (1995a)

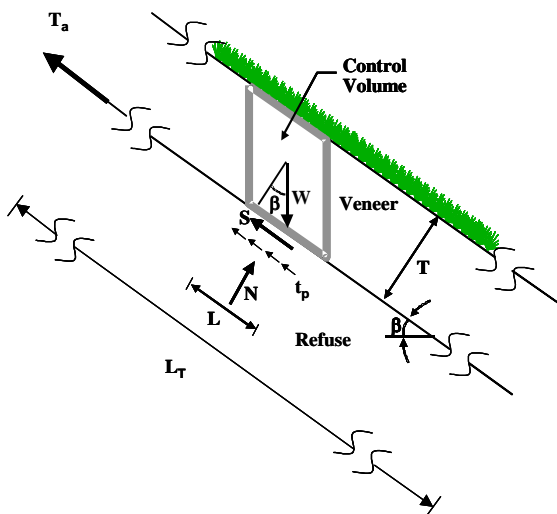


Figure 4. Veneer reinforced with uniaxial geosynthetic parallel to the slope

proposed method, the factor of safety is obtained by solving a quadratic equation. Koerner and Soong (1998) also provide analytical framework to address cases involving construction equipment, seepage forces, seismic forces, and the stabilizing effects of toe berms, tapered slopes and slope reinforcements. Thiel and Stewart (1993) and Punyamurthula and Hawk (1998) provide additional information regarding stability analysis of steep liner systems.

While a two-dimensional wedge analysis has been typically used in design, a simple one-dimensional analysis facilitates comparison with other reinforcement alternatives (e.g. fiber-reinforcement).

Figure 4 shows the one-dimensional case of a liner system reinforced using uniaxial geosynthetics placed parallel to the slope. In an infinite slope case, the shear force needed for equilibrium of the control volume is smaller than the one in the unreinforced case. In this case, the shear force is defined by:

$$S = W \sin \beta - t_p L \quad (7)$$

where  $t_p$  = distributed reinforcement tensile stress of the reinforcement parallel to the slope. When the geosynthetic reinforcements are placed parallel to the slope, the distributed reinforcement tensile stress can be

obtained by considering a uniform load transfer of the allowable reinforcement tensile strength ( $T_a$ ) along the total slope length ( $L_T$ ). Note that the length of the slope,  $L_T$ , is used to determine the distributed reinforcement tensile stress, even though the length is long enough as this is still a one-dimensional stability analysis. The distributed reinforcement tensile stress is defined as follows:

$$t_p = \frac{T_a}{L_T} \tag{8}$$

Table 1. Effect of different terms in the factor of safety estimated using Giroud et al. (1995a) methodology (adapted from Giroud et al. 1995a)

| Slope             | Infinite slope                   |                                  | Additional terms for finite slope   |  |                             |
|-------------------|----------------------------------|----------------------------------|---|--|-----------------------------|
| Mechanism         | Interface shear                  |                                  | Toe buttressing   |  | Geosynthetic                |
| Parameter         | Interface friction               | Interface adhesion               | Soil internal friction  | Soil cohesion  | Geosynthetic tension        |
| Symbol            | $\delta$                         | $a$                              | $\phi$  | $c$  | $T_a$                       |
| Factor of safety  | $\frac{\tan \delta}{\tan \beta}$ | $+\frac{a}{\gamma T \sin \beta}$ | $+\frac{T \tan \phi / (2 \sin \beta \cos^2 \beta)}{H_T (1 - \tan \beta \tan \phi)}$ | $+\frac{c}{\gamma H_T} \frac{1 / (\sin \beta \cos \beta)}{1 - \tan \beta \tan \phi}$ | $+\frac{T_a}{\gamma H_T T}$ |
| $\phi \nearrow$   | $\Leftrightarrow$                | $\Leftrightarrow$                | $\nearrow$  | $\nearrow$   | $\Leftrightarrow$           |
| $\beta \nearrow$  | $\searrow$                       | $\searrow$                       | $\searrow$  | $\searrow$   | $\Leftrightarrow$           |
| $h \nearrow$      | $\Leftrightarrow$                | $\Leftrightarrow$                | $\searrow$  | $\searrow$   | $\searrow$                  |
| $\gamma \nearrow$ | $\Leftrightarrow$                | $\searrow$                       | $\Leftrightarrow$   | $\searrow$   | $\searrow$                  |
| $t \nearrow$      | $\Leftrightarrow$                | $\searrow$                       | $\nearrow$  | $\Leftrightarrow$  | $\searrow$                  |

Notes:  $H_T$ : Total height of the slope;  $T_a$ : Allowable tensile strength of geosynthetic reinforcement  
 Influence on FS:  $\nearrow$  increasing;  $\Leftrightarrow$  no influence;  $\searrow$  decreasing;

From equations 2, 4, 5, 7 and 8, the factor of safety for the parallel-reinforcement case,  $FS_{r,p}$ , can be estimated as:

$$FS_{r,p} = \frac{\frac{c}{\gamma T \sin \beta} + \frac{\tan \phi}{\tan \beta}}{1 - \frac{t_p}{\gamma T \sin \beta}} \tag{9}$$

The equation above can be simplified by defining the normalized distributed reinforcement tensile stress  $t_p^*$  (dimensionless), as follows:

$$t_p^* = \frac{t_p}{\gamma T} \tag{10}$$

Combining Equations 6, 9, and 10:

$$FS_{r,p} = \frac{FS_u}{1 - t_p^* \frac{1}{\sin \beta}} \tag{11}$$

Equation 11 provides a convenient expression for stability evaluation of reinforced veneer slopes. It should be noted that  $FS_{r,p} = FS_u$  if the distributed reinforcement tensile stress  $t$  equals zero (i.e. in the case of unreinforced veneers). A case history involving the

use of geogrid reinforcement parallel to the liner slope is provided next. Additional case histories involving this type of veneer reinforcement are described by Baltz et al. (1995) and Martin and Simac (1995).

### Case History: McColl Superfund site, Fullerton, California

This project is a good example of a site where multiple systems of soil reinforcement were used for stabilization of the final cover system. One of these uses involves placements of geogrids along the cover system. The project also included the construction of conventional reinforced structures (Collins et al. 1998, Hendricker et al. 1998).

The site involves twelve pits containing petroleum sludge and oil-based drilling muds. The sludge was generated by the production of high-octane aviation fuel and were placed in the pits between 1942 and 1946. Between 1952 and 1964, the site was used for disposal of oil-based drilling muds. These wastes and their reaction products and byproducts were found as liquid, gas and solid phases within the pits. At the time of deposition, essentially all of the waste materials were mobile. Over time, much of the waste had hardened. The drilling mud is a thixotropic semi-solid sludge, which can behave as a very viscous fluid.

Key considerations for the selection of the final remedy were to: (i) provide a cover system that includes a barrier layer and a gas collection and treatment system over the pits to minimize infiltration of water and release of hazardous or malodorous gas emissions; (ii) provide a subsurface vertical barrier around the pits to minimize outward lateral migration of mobile waste or waste byproducts and inward lateral migration of subsurface liquid; and (iii) provide slope stability improvements for unstable slopes at the site.

The geogrid reinforcement for the cover system over the more stable pits was constructed with two layers of uniaxial reinforcement placed orthogonally to one another. Connections at the end of each geogrid roll were provided by Bodkin joints. Adjacent geogrid panels did not have any permanent mechanical connections. This was found to be somewhat problematic, as additional care was required during placement of the overlying gas collection sand to minimize geogrid separation. Details of the cover system involving geogrid reinforcement are shown in Figure 5.

A geocell reinforcement layer was constructed over the pits containing high percentages of drilling mud. While the construction of this reinforcement layer proceeded at a slower pace than the geogrid reinforcement, it did provide an immediate platform to support load. As the bearing capacity of the underlying drilling mud was quite low, the geocell provided

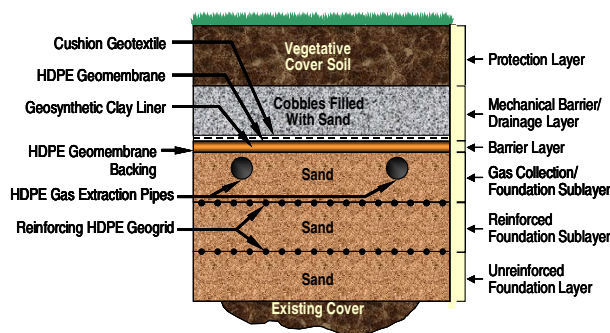


Figure 5. Cover system reinforced using uniaxial geogrids

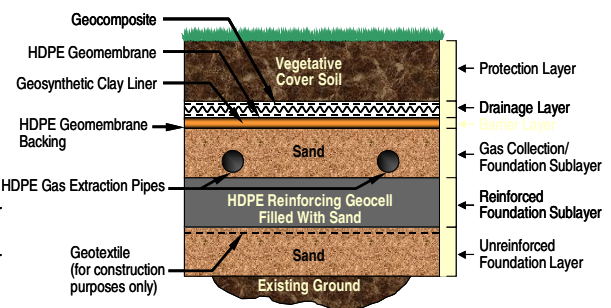


Figure 6. Cover system reinforced using geocells

load distribution, increasing the overall bearing capacity of the cover system. Details of the cover system involving geogrid reinforcement are shown in Figure 6.

In addition to reinforced covers, three conventional reinforced soil structures were constructed at the site. One of the structures was necessary to provide a working pad for construction of the subsurface vertical barrier. This reinforced earth structure had to support the excavator with a gross operating weight of 1,100 kN that was used to dig the soil-

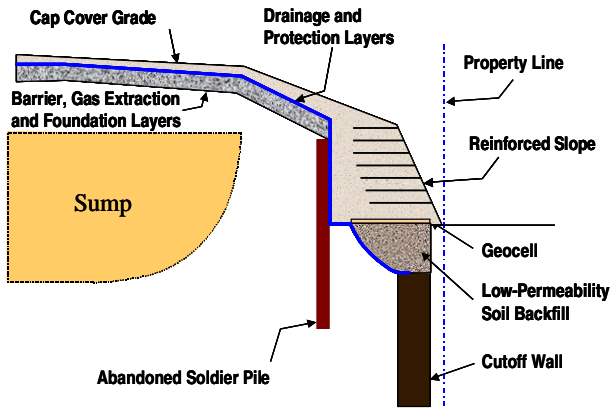


Figure 7. Buttressing reinforced slope at McColl Superfund site

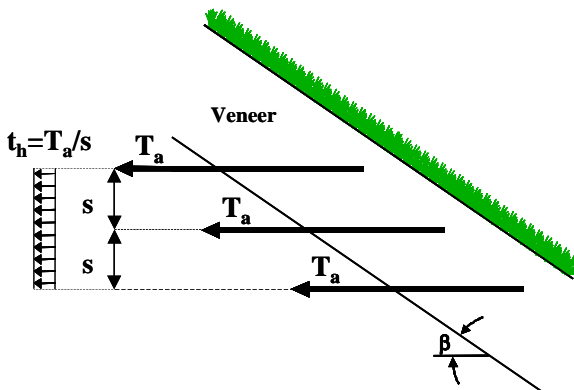
bentonite cutoff wall. Another reinforced earth structure at the site had to span a portion of completed cutoff wall. Due to concerns that the stress of the reinforced earth structure on the underlying soil-bentonite cutoff wall would lead to excessive deformation of the wall due to consolidation of the cutoff wall backfill, a flexible wall fascia was selected. As shown in Figure 7, a soldier pile wall was constructed to provide stability of the system during construction. The use of geosynthetic alternatives in this project was more suitable and cost effective than their conventional counterparts.

## LINERS REINFORCED WITH HORIZONTAL UNIAXIAL GEOSYNTHETICS

### General Approach

Figure 8 illustrates a liner (vener) reinforced using horizontally placed geosynthetics anchored into solid waste. Also in this case, the shear and normal forces acting on the control volume are defined not only as a function of the weight of the control volume, but also as a function of the tensile forces that develop within the reinforcements. For the purpose of the analyses presented herein, the reinforcement tensile forces are represented by a distributed reinforcement tensile stress  $t_h$ , which corresponds to a uniformly distributed tensile force per unit height. For a slope with reinforcement layers with uniform vertical spacing,  $t_h$  can be expressed by:

$$t_h = \frac{T_a}{s} \quad (12)$$



where  $T_a$  = allowable tensile strength of the reinforcement and  $s$  = vertical spacing between the layers. In this case, the shear and normal forces needed for equilibrium of a control volume are defined by:

$$S = W \sin \beta - t_h L \sin \beta \cos \beta \quad (13)$$

$$N = W \cos \beta + t_h L \sin^2 \beta \quad (14)$$

Figure 8. Vener reinforced with horizontal uniaxial geosynthetics

From Equations 2, 5, 12, 13, and 14 the following expression can be obtained for the factor of safety  $FS_{r,h}$  of a veneer reinforced with horizontal uniaxial geosynthetics:

$$FS_{r,h} = \frac{\frac{c}{\gamma T \sin \beta} + \frac{\tan \phi}{\tan \beta} + \frac{t_h}{\gamma T} \sin \beta \tan \phi}{1 - \frac{t_h}{\gamma T} \cos \beta} \quad (15)$$

The equation above can be simplified by defining the normalized distributed reinforcement tensile stress  $t_h^*$  (dimensionless), as follows:

$$t_h^* = \frac{t_h}{\gamma T} \cos \beta \quad (16)$$

Combining Equations 6, 15, and 16:

$$FS_{r,h} = \frac{FS_u + t_h^* \tan \beta \tan \phi}{1 - t_h^*} \quad (17)$$

Equation 17 provides a convenient expression for stability evaluation of reinforced veneer slopes. It should be noted that  $FS_r = FS_u$  if the distributed reinforcement tensile stress  $t_h$  equals zero (i.e. in the case of unreinforced veneers).

Additional aspects that should be accounted for in the design of reinforced veneer slopes include the evaluation of the pullout resistance (i.e. embedment length into the underlying mass), assessment of the factor of safety for surfaces that get partially into the underlying mass, evaluation of reinforcement vertical spacing, and analysis of seismic stability of the reinforced veneer. The case history described below illustrates the implementation of a horizontally-reinforced liner system.

### **Case History: North Slopes at OII Superfund site, Monterey Park, California**

A cover reinforced using horizontally placed geogrids was constructed as part of the final closure of the Operating Industries, Inc. (OII) landfill. This case history highlights the final closure of a hazardous waste landfill where the severe site constraints were overcome by designing and constructing an alternative final cover incorporating horizontal geosynthetic veneer reinforcement (Zornberg et al. 2001).

The 60-hectare south parcel of the OII landfill was operated from 1948 to 1984, receiving approximately 30-million cubic meters of municipal, industrial, liquid and hazardous wastes. In 1986, the landfill was placed on the National Priorities List of Superfund sites. Beginning in 1996, the design of a final cover system consisting of an alternative evapotranspirative soil cover was initiated, and subsequent construction was carried out from 1997 to 2000. The refuse prism, which occupies an area of about 50 hectares, rises approximately 35 m to 65 m above the surrounding terrain. Slopes of varying steepness surround a relatively flat top deck of about 15 hectares.

The final cover design criteria mandated by the U.S. Environmental Protection Agency (EPA) had to satisfy criteria for percolation performance, static and seismic stability of the steep sideslopes of the landfill, and erosion control. Stability criteria required a static factor

of safety of 1.5, and acceptable permanent seismically induced deformations less than 150 mm under the maximum credible earthquake. The basis of the seismic stability criteria is that some limited deformation or damage may result from the design earthquake, and that interim and permanent repairs would be implemented within a defined period.

One of the most challenging design and construction features of the project was related to the north slope of the landfill. The north slope is located immediately adjacent to the heavily traveled Pomona freeway (over a distance of about 1400 meters), rises up to 65 meters above the freeway, and consists of slope segments as steep as 1.5:1 (H:V) and up to 30 m high separated by narrow benches. The toe of the North Slope and the edge of refuse extends up to the freeway. The pre-existing cover on the North Slope consisted of varying thickness (a few centimeters to several meters) of non-engineered fill. The cover included several areas of sloughing instability, chronic cracking and high level of gas emissions. The slope was too steep to accommodate a layered final cover system, particularly a cover incorporating geosynthetic components (geomembranes or GCL).

After evaluating several alternatives, an evapotranspirative cover incorporating geogrid reinforcement for veneer stability was selected. The evapotranspirative cover had additional advantages over traditional layered cover systems, including superior long-term percolation performance in arid climates, ability to accommodate long-term settlements, good constructability, and ease of long-term operations and maintenance. The selected cover system included the following components, from the top down: 1) vegetation to promote evapotranspiration and provide erosion protection; 2) a 1.2 m – thick evapotranspirative soil layer to provide moisture retention, minimize downward migration of moisture, and provide a viable zone for root growth; and 3) a foundation layer consisting of soil and refuse of variable thickness to provide a firm foundation for the soil cover system.

Stability analyses showed that for most available evapotranspirative materials, compacted to practically achievable levels of relative compaction on a 1.5:1 slope (e.g. 95% of Standard Proctor), the static and seismic stability criteria were not met. Veneer geogrid reinforcement with horizontally placed geogrids was then selected as the most appropriate and cost-effective method for stabilizing the North Slope cover. Figure 9 shows the typical veneer reinforcement detail selected based on the shear strength of the soils used in construction.

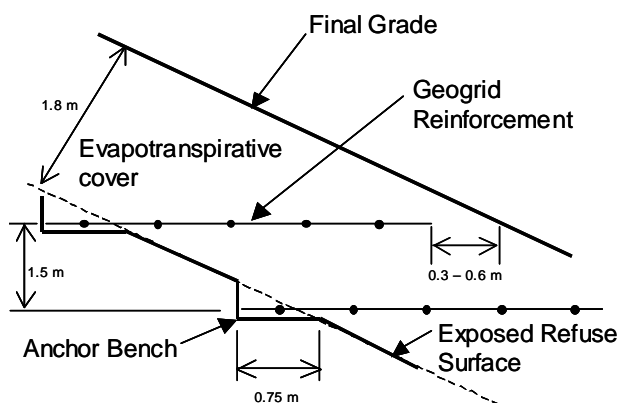


Figure 9. Typical reinforcement detail for horizontal reinforcement anchored into solid waste (from Zornberg et al. 2001)

The veneer reinforcement consisted of polypropylene uniaxial geogrids, installed at 1.5-m vertical intervals for slopes steeper than 1.8:1, and at 3-m vertical intervals for slopes between 2:1 and 1.8:1. The geogrid panels are embedded a minimum of 0.75 m into the exposed refuse slope face from which the pre-existing cover had been stripped. The geogrid panels were curtailed approximately 0.3 to 0.6 m away from the finished surface of the slope cover. This was done to permit surface construction, operation and maintenance activities on

the slope face without the risk of exposing or snagging the geogrid.

Construction of the North Slope was completed in 12 months. Approximately 500,000 m<sup>3</sup> of soil and 170,000 m<sup>2</sup> of geogrid were placed. Total area of geogrid placement exceeded 9.3 hectares. The maximum height of reinforced portion of the landfill slopes was 55 m (the maximum height of the total landfill slope was 65 m).

## **LINERS REINFORCED WITH RANDOMLY DISTRIBUTED FIBERS**

### **General Approach**

A promising alternative for stabilization of steep landfill liners involves the use of fiber-reinforcement. Advantages of fiber-reinforcement over planar reinforcement in the stabilization of landfill liners are:

- Fiber-reinforcement is particularly suitable for stabilization of veneer slopes, as it provides additional shear strength under low confining pressures. A small increase of shear strength under low confinement has a significant impact on the stability of shallow slopes.
- Randomly distributed fibers helps maintaining strength isotropy and do not induce potential planes of weakness that can develop when using planar reinforcement elements.
- No anchorage is needed into solid waste as in the case of reinforcement with horizontal geosynthetics or at the crest of the slope as in the case of reinforcement parallel to the landfill slope.
- In addition to stabilizing the liner slopes, fiber reinforcement has the potential of mitigating the potential for crack development, providing erosion control, and facilitating the establishment of vegetation.

Relevant contributions have been made towards the understanding of the behavior of fibers (Gray and Al-Refeai 1986; Bouazza and Amokrane 1995). Potential advantages of fiber-reinforced solutions over the use of other slope stabilization technologies have been identified, for example, for slope repairs in transportation infrastructure projects (Gregory and Chill 1998) and for the use of recycled and waste products such as shredded tires in soil reinforcement (Foose et al. 1996). Micro-reinforcement techniques for soils also include the use of “Texol”, which consists of monofilament fibers injected randomly into sand (Leflaive 1985) and the use of randomly distributed polymeric mesh elements (McGown et al. 1985; Morel and Gourc 1997). The use of fiber-reinforced clay backfill to mitigate the development of tension cracks was evaluated by Al Wahab and El-Kedrah (1995) and by Maher and Ho (1994). Several composite models have been proposed in the literature to explain the behavior of randomly distributed fibers within a soil mass. The proposed models have been based on mechanistic approaches (Maher and Gray 1990), on energy dissipation approaches (Michalowski and Zhao 1996), and on statistics-based approaches (Ranjar et al. 1996).

Fiber-reinforced soil has often been characterized as a single homogenized material, with properties defined using laboratory testing of composite fiber-reinforced soil specimens. However, the need for laboratory characterization of composite specimens has

been a major drawback in the implementation of fiber-reinforcement in soil stabilization projects. To overcome this difficulty, a discrete approach that characterizes the fiber-reinforced soil as a two-component (fibers and soil) material was recently developed (Zornberg 2002). The main features of this approach are:

- The reinforced mass is characterized by the mechanical properties of individual fibers and of the soil matrix rather than by the mechanical properties of the fiber-reinforced composite.
- A critical confining pressure at which the governing mode of failure changes from fiber pullout to fiber breakage can be defined using the individual fiber and soil matrix properties.
- The fiber-induced distributed tension is a function of fiber content, fiber aspect ratio, and interface shear strength of individual fibers if the governing mode of failure is by fiber pullout.
- The fiber-induced distributed tension is a function of fiber content and ultimate tensile strength of individual fibers if the governing mode of failure is by fiber breakage.
- The discrete framework can be implemented into an infinite slope limit equilibrium framework. Convenient expressions can be obtained to estimate directly the required fiber content to achieve a target factor of safety.

The design methodology for fiber-reinforced soil structures using a discrete approach is consistent with current design guidelines for the use of continuous planar reinforcements and with the actual soil improvement mechanisms. Consequently, fiber-reinforced liner systems are expected to lead to economically and technically superior alternatives for reinforcement of landfill liners.

Figure 10 shows a schematic view of a fiber-reinforced infinite slope. The behavior of the fiber-reinforced soil mass depends on whether the failure mode is governed by pullout or breakage of the fibers. The governing failure mode of the fiber-reinforced soil mass depends on the confinement. A critical normal stress,  $\sigma_{n,crit}$ , can be defined for comparison with the normal stress  $\sigma_n$  at the base of the veneer. If  $\sigma_n < \sigma_{n,crit}$ , the dominant mode of failure is the fibers pullout. This is the case for liner system applications. In this case, the fiber-induced distributed tension  $t_f$  is defined by (Zornberg 2002):

$$t_f = \eta \chi c_{i,c} c + \eta \chi c_{i,\phi} \tan \phi \sigma_n \quad (18)$$

where  $c_{i,c}$  and  $c_{i,\phi}$  are the interaction coefficients for the cohesive and frictional components of the interface shear strength;  $\eta$  = aspect ratio (length/diameter) of the individual fibers, and  $\chi$  = volumetric fiber content.

Similarly, if  $\sigma_n > \sigma_{n,crit}$ , the dominant mode of failure is fiber breakage. Even though this is not generally the governing

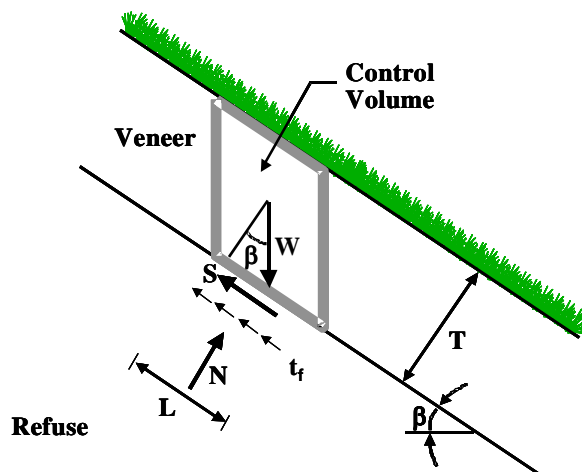


Figure 10. Veneer reinforced with randomly

mode of failure for cover slopes the solution for this case is presented for completeness. The fiber-induced distributed tension  $t_f$  is defined by:

$$t_f = \sigma_{f,ult} \cdot \chi \quad (19)$$

where  $\sigma_{f,ult}$  = ultimate tensile strength of the individual fiber.

In a fiber-reinforced veneer, the shear force needed for equilibrium of the control volume equals:

$$S = W \sin \beta - \alpha t_f L \quad (20)$$

where  $\alpha$  is an empirical coefficient that accounts for preferential orientation of fibers. For the case of randomly distributed fibers considered herein  $\alpha$  equals one.

Using Equations 4, 5, 18, and 20 into Equation 2 leads to the factor of safety for a fiber-reinforced veneer,  $FS_{r,f}$ :

$$FS_{r,f} = \frac{\frac{c}{\gamma T \sin \beta} + \frac{\tan \phi}{\tan \beta}}{1 - \frac{\alpha t_f}{\gamma T \sin \beta}} \quad (21)$$

The normalized distributed reinforcement tensile stress  $t_f^*$  (dimensionless) of a fiber-reinforced slope can be defined as follows:

$$t_f^* = \frac{t_f}{\gamma T} \quad (22)$$

Combining Equations 6, 21, and 22 leads to the following definition of the factor of safety:

$$FS_{r,f} = \frac{FS_u}{1 - \alpha t_f^* \frac{1}{\sin \beta}} \quad (23)$$

### Case History: Redwood Landfill, Redwood City, California

A stabilization project was completed in October 2003 using fiber-reinforced soil for the base liner at Redwood Landfill, Area G, Phase 1 in Marin County, California (Minch, 2004). Waste Management is the owner of the site, RJ Gordon Construction was the contractor, and GeoSyntec Consultants was the designer of the cell.

The project involved stabilization of a base liner system using fibrillated polypropylene fibers placed at a dosage of 0.1 %. The main objective of using fibers in this project was to increase the interface friction angle between the clay liner and a textured geomembrane. The liner was constructed using San Francisco Bay Mud, which is characterized by very low shear strength. Accordingly, polypropylene fibers were used to allow steepening of the side slopes in the facility. An experimental testing program was conducted to evaluate the benefit of using fibers in the clay liner. The laboratory test results were reported to provide a significant increase in interface friction angle when using fibers. Such increase in shear strength was attributed to a “Velcro-like” effect between the fibrillated fibers and the

textured geomembrane (Chill, 2004). In addition to increasing the interface shear strength between Bay Mud and textured geomembrane, the use of fibers led to an increase in the internal friction angle of the clay liner itself.

The implementation of fiber-reinforcement allowed increasing the originally planned liner slope of 5:1 to a slope of 3:1. Such design change resulted in significant cost savings and additional airspace. Figure 11 shows a typical cross section of the base containment system at Redwood Landfill. As shown in the figure, the upper 0.30 m (6 inches) of the low-hydraulic conductivity soil layer was reinforced with fibers placed at a dosage of 0.1%. The liner system includes a single composite liner with an 80-mil HDPE double-sided textured geomembrane placed over a 0.6 m (2 ft) thick low-hydraulic conductivity layer. The system also includes a granular liquid collection layer over the composite liner and an underdrain collection layer constructed underneath the liner. Nonwoven geotextiles are used for filtration and separation purposes above and below each of the granular drainage layers.

The potential impact of the polypropylene fibers on the hydraulic conductivity of the clay liner material was also evaluated as part of the experimental testing program. The experimental results were reported to demonstrate that the hydraulic conductivity obtained for the fiber-reinforcement Bay Mud remained below  $10^{-7}$  cm/sec, which is the maximum hydraulic conductivity value specified in the design criteria.

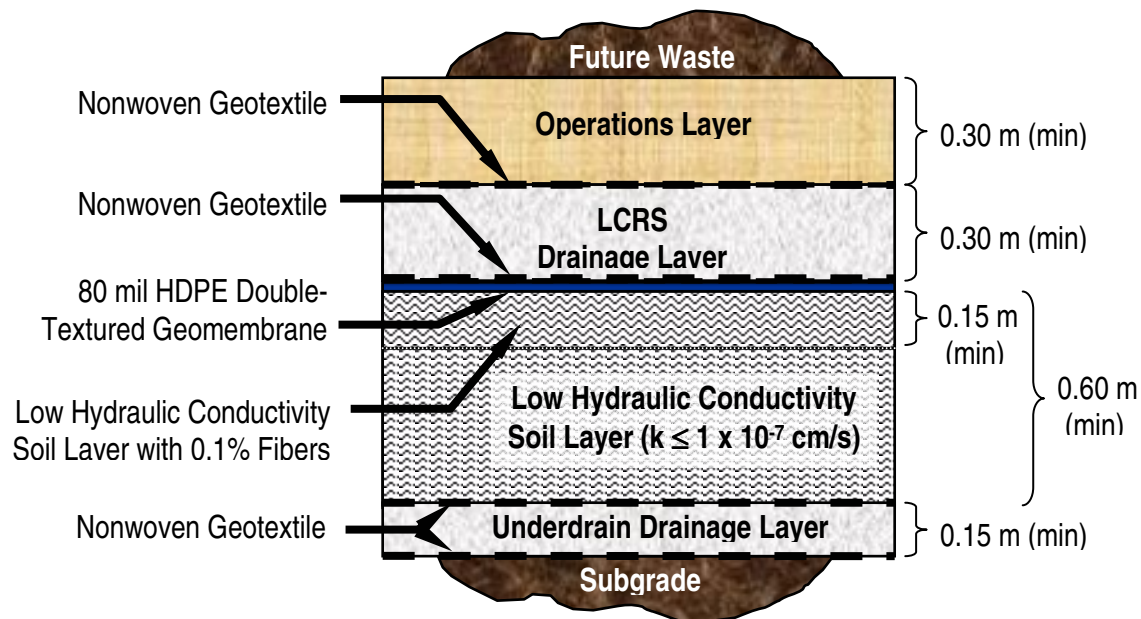


Figure 11. Typical cross-section of the fiber-reinforced base liner at Redwood Landfill, CA

### COMPARISON AMONG DIFFERENT APPROACHES FOR LINER STABILITY

The use of a consistent framework for comparison of different reinforcement approaches for liner systems facilitates the evaluation of design alternatives. This is because the different veneer reinforced methodologies consider a consistent definition for the factor of safety (Equation 1). Solutions are presented for the case of unreinforced, parallel-

reinforced, horizontally-reinforced and fiber-reinforced veneers. Table 2 summarizes the expressions for the factor of safety in each case and the influence of the parameters governing the stability of the liner. As expected, the use of reinforcement always leads to an increased factor of safety in relation to the unreinforced case. This is reflected in the table by the fact that an increased normalized reinforcement tension  $t^*$  always leads to an increased factor of safety. As also expected, an increased slope inclination  $\beta$  leads to decreasing factor of safety. However, it is worth noting that increasing soil friction angle (e.g. by densifying the soil liner material) leads to an increased normalized reinforcement tension  $t^*$  only for the case of fiber reinforced slopes. That is, the soil friction angle affects  $t_f$  (Equation 18), but does not affect  $t_p$  (Equation 8) nor  $t_h$  (Equation 12). It should also be noted that an increased total height of the slope  $H_T$  (or increased total length  $L_T$ ) does not affect detrimentally the efficiency of horizontally placed reinforcements and of fiber reinforcement.

Table 2. Effect of different terms in the factor of safety of liner systems using different reinforcement approaches

| Definition of Factor of Safety  |   | Influence on the factor of safety compared to $FS_u$ |         |        |                |
|---------------------------------|---|--|---------|--------|----------------|
|                                 |   | $t^*$  | $\beta$ | $\phi$ | $L_T$ or $H_T$ |
| Unreinforced veneer             | $FS_u = \frac{c}{\gamma T \sin \beta} + \frac{\tan \phi}{\tan \beta}$       |  |         |        |                |
| Reinforcement parallel to slope | $FS_{r,p} = \frac{FS_u}{1 - t_p^* \frac{1}{\sin \beta}}$                    | with $t_p^* = \frac{t_p}{\gamma T}$                  | ↗       | ↘      | ↔              |
| Horizontal reinforcement        | $FS_{r,h} = \frac{FS_u + t_h^* \sin \beta \tan \phi}{1 - t_h^* \cos \beta}$ | with $t_h^* = \frac{t_h}{\gamma T}$                  | ↗       | ↘      | ↔              |
| Fiber-reinforcement             | $FS_{r,f} = \frac{FS_u}{1 - \alpha t_f^* \frac{1}{\sin \beta}}$             | with $t_f^* = \frac{t_f}{\gamma T}$                  | ↗       | ↘      | ↔              |

Notes:  $t_p$  = distributed tensile stress per unit length of a liner with reinforcement parallel to the slope (Equation 8)  
 $t_h$  = distributed tensile stress per unit height of a liner with horizontal reinforcement (Equation 12)  
 $t_f$  = distributed tensile stress per unit length of a liner with fiber-reinforcement (Equation 18)  
 Influence on FS: ↗ increasing; ↔ no influence; ↘ decreasing.

## SUMMARY AND CONCLUSIONS

Innovative approaches have been recently implemented in the US involving the use of geosynthetic reinforcements in final cover and base liner systems. In particular, design approaches have involved the design of conventional reinforced soil structures subjected to significant differential settlements as well as reinforced veneers using geosynthetic reinforcements parallel to the slope, horizontal geosynthetic reinforcements anchored into solid waste, and fiber reinforcement.

The use of conventional geosynthetic-reinforced soil structures (e.g. at the toe of cover slopes) as well as the use of geosynthetic reinforcements placed parallel to the liner slope have been implemented in the US for the last twenty years. The design of conventional reinforced soil structures does not differ from the design of these systems for other applications such as transportation infrastructure. It should be noted, however, that these reinforced soil structures are often founded on highly compressible waste material. Conventional reinforced soil structures have shown to perform excellently even when subjected to major differential settlements. Veneer reinforcement using geosynthetics

placed parallel to the liner slopes is a well-established alternative in the US, and is suitable for stabilization of liner slopes. However, this approach can be unsuitable for comparatively long and/or steep slopes because of the high tensile strength requirements needed for such cases.

The use of fiber-reinforcement and of horizontally-placed reinforcements for stabilization of veneer slopes has been recently implemented in the US. As expected, additional reinforcement always leads to a higher factor of safety while increasing slope inclination leads to decreasing stability. However, it should be noted that increasing soil friction angle leads to an increased normalized reinforcement tension only for the case of fiber reinforced slopes. It should also be noted that increasing total height of the slope (or increasing total length) does not affect detrimentally the efficiency of horizontally placed reinforcements and of fiber reinforcement.

Excellent field performance has been reported in case histories involving the use of conventional reinforced soil structures in landfill projects as well as in the case of liners reinforced using geosynthetics placed parallel to the slope, using geosynthetics placed horizontally and anchored into solid waste, or using fiber reinforcement.

#### **ACKNOWLEDGEMENTS**

The author is grateful to Glen Roycroft of Waste Management and Michael Minch of GeoSyntec Consultants for the information provided on the Redwood Landfill case history.

#### **REFERENCES**

- Al Wahab, R.M. and El-Kedrah, M.M. 1995. Using fibers to reduce tension cracks and shrink/swell in compacted clays. *Geoenvironment 2000, ASCE Geotechnical Special Publication*, 46: 433-446.
- Baltz, J. F., Zamojski, L. and Reinknecht, D. 1995. Design and construction of a geogrid-reinforced veneer landfill cap. *Proceedings Geosynthetics '95 Conference, Nashville*, 759-770.
- Bouazza, A. and Amokrane, K. 1995. Granular soil reinforced with randomly distributed fibres. *Proceedings 11<sup>th</sup> African Regional Conference on Soil Mechanics and Foundation engineering, Cairo*. 207-216.
- Bouazza, M., Zornberg, J.G., and Adam, D. 2002. "Geosynthetics in Waste Containment Facilities: Recent Advances." Keynote paper, *Proceedings of the Seventh International Conference on Geosynthetics, Nice, France, 22-27 September, A.A. Balkema, Vol. 2, pp. 445-510.*
- Cargill, K.W. and Olen, K.L. 1998. Landfill closure using reinforced soil slopes. *Proceedings 6th International Conference on Geosynthetics, Atlanta*, 481-486
- Chill, D. 2004. Personal communication.
- Collins, P., Ng, A.S. and Ramanujam, R. 1998. Superfund success, superfast. *Civil Engineering, December*, 42-45.
- Foose, G.J., Benson, C.H. and Bosscher, P.J. 1996. Sand reinforced with shredded waste tires. *Journal of Geotechnical Engineering*, 122 (9): 760-767.
- Giroud, J.P., Williams, N.D., Pelte, T. and Beech, J.F. 1995a. Stability of geosynthetic-soil layered systems on slopes. *Geosynthetics International*, 2(6): 1115-1148

- Giroud, J.P., Bachus, R.C. and Bonaparte R. 1995b. Influence of water flow on the stability of geosynthetic-soil layered systems on slopes. *Geosynthetics International*, 2(6): 1149-1180
- Gray, D.H. and Al-Refeai, T. 1986. Behaviour of fabric versus fiber-reinforced Sand. *Journal of Geotechnical Engineering*, 112(8): 804-820.
- Gregory, G. H. and Chill, D. S. 1998. Stabilization of earth slopes with fiber-reinforcement. *Proceedings 6<sup>th</sup> International Conference on Geosynthetics, IFAI, Atlanta*, Vol. 2, 1073-1078.
- Hendricker, A.T., Fredianelli, K.H., Kavazanjian, E. and McKelvey, J.A. 1998. Reinforcement requirements at a hazardous waste site. *Proceedings 6<sup>th</sup> International Conference on Geosynthetics. IFAI, Atlanta*, Vol. 1, 465-468.
- Koerner, R.M. and Soong, T.Y. 1998. Analysis and design of veneer cover soils. *Proceedings 6<sup>th</sup> International Conference on Geosynthetics, Atlanta*, Vol. 1: 1-23.
- Leflaive, E. 1985. Soils reinforced with continuous yarns: the Texol. *Proceedings 11<sup>th</sup> International Conference On Soil Mechanics and Foundation Engineering, San Francisco*, Vol. 3: 1787-1790.
- Maher, M.H. and Gray, D.H. 1990. Static response of sand reinforced with randomly distributed fibers. *Journal Geotechnical Engineering*, 116(1): 1661-1677.
- Maher, M. H. & Ho, Y. C. 1994. Mechanical properties of kaolinite/fiber soil composite. *ASCE J. Geotech. Engng.*, 120, No. 8, 1381-1393.
- Martin, J. S. and Simac, M. R. 1995. The design and construction of 168 meter-long geogrid reinforced slopes at the Auburn, NY, landfill close. *Proceedings Geosynthetics '95 Conference, Nashville*, 771-784.
- McGown, A., Andrawes, K.Z, Hytiris, N. and Mercel, F.B. 1985. Soil strengthening using randomly distributed mesh elements. *Proceedings 11<sup>th</sup> International Conference On Soil Mechanics and Foundation Engineering, San Francisco*, Vol. 3: 1735-1738.
- Michalowski, R.L. and Zhao, A. 1996. Failure of fiber-reinforced granular soils. *Journal Geotechnical Engineering*, 122(3): 226-234.
- Minch, M. 2004. Personal communication.
- Morel, J.C. and Gourc, J.P. 1997. Mechanical behavior of sand reinforced with mesh elements. *Geosynthetics International*, 4(5): 481-508.
- Punnamurthula, S. and Hawk, D. 1998. Issues with Slope Stability of Landfill Cover Systems. *Proceedings 12<sup>th</sup> GRI Conference, Folsom*, 259-268.
- Ranjan, G., Vassan, R.M. and Charan, H.D. 1996. Probabilistic Analysis of Randomly Distributed Fiber-Reinforced Soil. *Journal Geotechnical Engineering*, 120(6): 419-426.
- Thiel, R.S. and Stewart, M.G. 1993. Geosynthetic landfill cover design methodology and construction experience in the pacific northwest. *Proceedings Geosynthetics 93 Conference, Vancouver*, 1131-1144.
- Zornberg, J.G. 2002. "Discrete Framework for Limit Equilibrium Analysis of Fibre-Reinforced Soil." *Géotechnique*, Vol. 52, No. 8, pp. 593-604.
- Zornberg, J.G. and Kavazanjian, E. 2001. Prediction of the performance of a geogrid-reinforced slope founded on solid waste. *Soils and Foundations*, 41(6): 1-16.
- Zornberg, J.G., Somasundaram, S. and LaFountain, L. 2001. Design of Geosynthetic-Reinforced Veneer Slopes. *Proceedings International Symposium on Earth Reinforcement: Landmarks in Earth Reinforcement, Fukuoka*, 305-310.